 doi:10.20944/preprints202109.0093.v1

Article

WRF evaluation during Storm Ophelia using remote sensing and in-situ measurements at Mace Head, Ireland.

School of Physics & Centre for Climate & Air Pollution Studies, National University of Ireland, Galway, Ireland.

Clare Noone[1], J. Preißler[2], R.-M. Hu, L. Coleman, P. Pandey, C. O´Dowd

[1] Affiliation 1; now at Maynooth University, clare.noone@mu.ie
[2] Affiliation 2; *now at Leosphere, Saclay, France*
* Correspondence: clare.noone@mu.ie

Abstract: Storm Ophelia made landfall over Ireland as an extra-tropical storm on the morning of the 16th October 2017. The storm caused major power outages, lifted roofs, caused coastal flooding in Ireland, and resulted in the loss of three lives. A model's capability to forecast extreme weather events such as Storm Ophelia is of upmost importance and now with a changing climate, it becomes more important to improve and enhance model forecasting capability. The Weather Research and Forecasting (WRF) model V3.9 has been configured for the Irish domain and this study presents a preliminary evaluation of the Model during Storm Ophelia. Simulated wind speed and direction were compared with hourly remote sensing (lidar) and in-situ (wind speed and wind direction at 10m) observations at the coastal site of Mace Head Atmospheric Research Station on the West coast of Ireland (53.33◦ N, 9.90 49 ◦ W). The model simulation has generally small biases in the simulated wind speed and wind direction during this case study. The model also realistically simulated the magnitude and geographical distribution of the wind speed and wind direction observed during Ophelia.

Keywords: WRF, Modelling, LIDAR,

1. Introduction

Earth's climate is rapidly changing, with widespread changes in the atmosphere, ocean, cryosphere, and biosphere [1]. Human-induced climate change is already affecting many weather and climate extremes in every region across the globe and there is more evidence of observed changes in extremes such as heatwaves, heavy precipitation, droughts, and tropical cyclones. Increasing likelihoods of extreme weather events is the most noticeable and damaging manifestation of human induced climate change [2]. Hurricanes are among the most devasting natural disasters, with approximately 80-90 tropical cyclones reaching tropical storm intensity around the globe [6]. The number of categories 3, 4, and 5 North Atlantic hurricanes during the first decade of the 21st century was the highest since 1951. The recent increases in activity are linked, in part, to higher sea surface temperatures in the region where Atlantic hurricanes form and move through. An increase in strength and number of intense hurricanes is projected for the end of this century. These projected changes are based on an average of projections from a number of individual high-resolution models and mechanistic considerations [3] [4] [5].

 doi:10.20944/preprints202109.0093.v1

Storm Ophelia was the easternmost major hurricane on record. It caused almost 70 million worth of damage and is considered to be the worst storm to affect Ireland in 50 years. The tropical storm developed from the strongest eastern Atlantic storm in a century and a half and brought wind speeds of 191 km/h to parts of Ireland. It left more than 385,000 homes without power, and effectively shut down the country for 2 days. Three deaths can be directly attributed to Ophelia, all of which occurred in Ireland. Figures 1(a) and 1(b) give an overview of the storm from satellite images. In Figure 1(b), the eye of the hurricane is clearly visible.

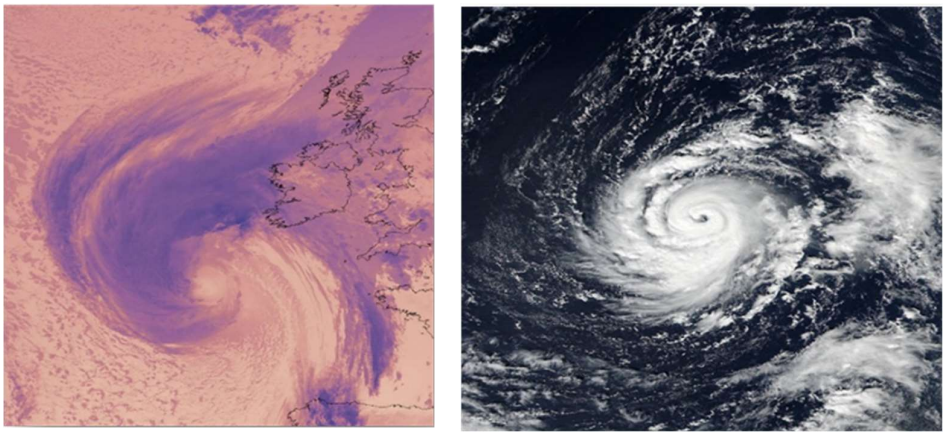

Figure 1: Images from NASA-NOAA's Suomi NPP satellite; (a) Thermal image of Hurricane Ophelia from over Ireland on Oct. 16 at 02:54 UTC; (b) Visible light image of Ophelia over the Atlantic on Oct. 12 at 15:30 UTC.

Current mesoscale numerical models, such as the Weather Research and Forecasting (WRF) model, are capable of simulating intense tropical cyclones with realistic structures [7]. The WRF Model is designed to serve both operational forecasting and atmospheric research needs [8][9][10]. Evaluation of the Hurricane Weather Research and Forecasting (HWRF) model, designed specifically for hurricane studies [11] against WRF Models showed that the intensity forecasts displayed only marginal improvement of 5–8 % over the operational forecasts [15]. Domain size, location, and resolution are critical [12][13] and the importance of selecting representative grid points for evaluating the model performance has been shown to be of relevance [14].

2. Materials and Methods

2.1 WRF model configuration

One of the essential steps in numerical weather forecasting simulations is the initial setup of physics options for the region and time period being considered. The mesoscale model used in this study is the Weather Research and Forecasting Model (WRF). WRF is a multi-scale model which scales from hemispheric scale down to km scale and can accommodate multiple levels of nesting. The WRF model is used extensively within academia, governments, and industry, and has an ability to simulate a wide range of synoptic scale, mesoscale, and microscale atmospheric phenomena. The model is equipped with multiple parameterization schemes (e.g., microphysics, land-surface interaction, radiation, planetary boundary layer, etc.) [7]. WRF can produce simulations based on actual atmospheric conditions (i.e., from observations and analyses) or idealized conditions. In this study simulations were carried out using 3 nested resolutions, 25km, 5km, and 1km. WRF Version 3.9 was used for model simulations. The centre of domain is located at 52.32N, 1.51W with a resolution of 25 km, which covers Ireland, UK, and most European

 doi:10.20944/preprints202109.0093.v1

regions. The vertical structure is divided into 30 levels, of which 8 levels are below 1 km altitude [10]. The terrain, land use and soil data are interpolated into model grids from the USGS global elevation with resolutions of 10 m, 2 m, and 30 m respectively. The European Centre for Medium-Range Weather Forecasts (ECMWF) Reanalysis (ERA) Interim data files are used for the meteorological initialization and boundary conditions [21]. The ERA-Interim ends on 31st August 2019. The ERA-Interim file needed to be interpolated to the limited area of WRF domain. This process is realised by the WRF Pre-Processing system (WPS). In addition, we use the RRTM shortwave radiation schemes [22], and the Unified Noah land surface model. The sub grid-scale turbulence mixing is turned on without explicit computational mixing. The microphysics and PBL schemes are Lin et al & YSU scheme [23]. The full model configuration used in this study is presented in Table 1.

	WRF MODEL SETUP
MODEL SOFTWARE VERSION	*V3.9*
NUMBER OF DOMAINS	*3 domains*
HORIZONTAL RESOLUTION	*1km, 5km and 25 km*
TEMPORAL RESOLUTION	*1 hour*
FORECAST IN HOURS	*87 hours*
NUMBER OF GRID POINTS	*100x111, 186x131, 191x141*
MAP PROJECTION	*lambert*
HORIZONTAL GRID	*Arakawa C-grid staggering [24]*
VERTICAL COORDINATE	*Hybrid sigma-pressure*
TIME INTEGRATION	*Runge-Kutta scheme*
MICROPHYSICS	*Lin et al. scheme*
RADIATION	*RRTM*
AEROSOL SCHEME	*no chemistry*
CHEMICAL MECHANISM	*no chemistry*
PLANETARY BOUNDARY LAYER (PBL)	*YSU scheme*
LAND –SURFACE PARAMETERIZATION	*Unified Noah land-surface scheme*
CUMULUS PARAMETERIZATION	*Grell-Devenyi ensemble scheme*

Table 1: WRF 3.9 model configuration used in this study.

2.2 Doppler Lidar Measurements

We validated WRF wind profiles using a scanning Doppler wind lidar of type WindCube 200S from manufacturer Leosphere (France). The lidar is located at Mace Head, about 300 m from the shoreline at 21 m above ground level. The scanning lidar delivers radial wind speed along any line of sight, from which horizontal wind speed and direction can be calculated using a specific scan pattern. At intervals of 15 minutes, conical scans at fixed elevation angles, also referred to as velocity-azimuth-display (VAD), were performed consisting of 12 beams at discreet azimuth angles 30° apart. The elevation angle of the conical scans used for this study was 15°. Temporal and vertical resolution of the resulting wind field was 15 minutes and 20 m.

To obtain horizontal wind speed and direction, radial wind values were fitted to a sine-curve as suggested by Browning and Wexler [33]. The least-square fit was applied to each range bin (horizontal cross section of the cone forming a circle). Availability of lidar signal depends on the presence of scatters, which are mostly aerosol particles. Therefore, low signal-to-noise ratios are common at altitudes above the boundary layer and lead to

poor fits, which we screened out by applying a threshold of the correlation coefficient R of the fit of 0.98. Besides, in this part of the study we focus on eight WRF height levels below 1300 m above sea level, to avoid outliers affecting the validation. For comparison of WRF and lidar profiles of wind speed and direction, the closest lidar altitude to the WRF levels, as well as the closest lidar time stamp to the full hour were selected.

2.3 Evaluation parameters

WRF model simulations from the three domains (D1), (D2) and (D3) were evaluated statistically against the near surface in situ observations measured by the automatic weather station. The investigated parameters were wind speed and wind direction. The capability of the model was evaluated for a 24-h forecast period starting from 0000 UTC to 0000 UTC the next day (the initial 12 h being discarded for model spin-up). Due to the complexity and uncertainty associated with the forecast verification process, it is well known that a single verification statistic cannot depict the quality of a forecast [34]. A number of standard qualitative and quantitative accuracy measures were used to assess the forecast, namely mean bias error (*MBE*), root mean square error (*RMSE*), standard deviation of the mean value (σ) and correlation coefficient (r).

3 WRF Model comparison to in-situ measurements

Our simulation period covers the time when Storm Ophelia reached Ireland, from 16 to 18 October 2017. In this section, model simulations for nested resolutions 25km, 5km, and 1km are compared against hourly in-situ Met Eireann measurements of wind speed and direction at Mace Head. Results using the metrics introduced in the previous section, for the 16 and 17 October are shown in Table 2.

	16/10/2017			***17/10/2017***	
	Mace Head centre wind speed				
WRF resolution	R2	RMSE	MBE	R2	RMSE
25 km	0.23	3.7	-1.46	0.90	3.1
5 km	0.11	2.8	-1.45	0.93	1.6
1 km	0.17	6.1	-6.81	0.94	5.8
	Mace Head centre wind direction				
WRF resolution	R2	RMSE	MBE	R2	RMSE
25 km	0.27	35	-35	0.78	37.8
5 km	0.54	24.5	-25	0.92	11.16
1 km	0.63	14.88	-19.9	0.75	5.88

Table 2: Comparison of WRF results with in-situ measured 10-m wind at Mace Head on 16 October 2017, Mace Head centred extracted point

Comparing wind direction and wind speed at 10m against WRF simulations on the 16 October shows poor agreement for wind speed, with R^2 smaller than 0.23 for all WRF resolutions. *MBE*, however, was small, especially for WRF resolution of 5 and 25 km. Wind direction compared better than wind speed, with R^2 ranged from 0.27-0.63 for the WRF resolutions, but *RMSE* and *MBE* were large. The comparison on 17 October shows excellent correlation for wind speed with R^2 between 0.90 and 0.94 for 25 km and 1 km resolution, respectively, and small *MBE* and *RMSE*. Wind direction agreed reasonably well, with R^2 between 0.75 and 0.92, and smaller *MBE* and *RMSE* than from the run-on 16 October.

	maximum wind speed m/s	*time of maximum UTC*
measured	18.5	07:00
WRF 25km	21.2	12:00
WRF 5 km	**17.8**	**08:00**
WRF 1 km	11.8	21:00

Table 3: Observed and forecasted wind speed maximum on 16 October, as well as time the maximum was recorded, Mace Hea

Table 3 shows maximum and medium wind speed, and the time the maximum wind speed was recorded, or forecasted by WRF. The nested WRF 5km resolution captures both, timing, and wind speed very well, forecasting the peak within 1 hour of the maximum hourly average wind speeds measured on 16 October. WRF 25km appears to have a time lag of several hours. While the WRF 1km resolution misses both the intensity and timing of the peak wind speeds.

4 WRF Model comparison to Lidar measurements

4.1 WRF & Lidar Wind speed (30 vertical levels)

For comparison of WRF and lidar profiles of wind speed, the closest lidar altitude to the WRF levels, as well as the closest lidar time stamp to the full hour were selected. Table 4 (A & B) show wind speed comparison results for 16 & 17 October 2017 for lidar VAD_15 and VAD_75.

WRF & LIDAR RESULTS MACE HEAD 16H OCTOBER 2017- WIND SPEED VAD_15

MODEL	**R**	**R 2**	**RMSE**	**Std Dev**
WRF (25KM)	0.59	0.35	7.62	0.11
WRF (5KM)	**0.68**	**0.46**	**5.42**	**0.08**
WRF (1KM)	0.67	0.45	6.44	0.09

WRF & LIDAR RESULTS MACE HEAD 16H OCTOBER 2017- WIND SPEED-VAD_75

MODEL	**R**	**R2**	**RMSE**	**Std Dev**
WRF (25KM)	**0.63**	**0.40**	**8.56**	**0.09**
WRF (5KM)	0.55	0.30	7.01	0.08
WRF (1KM)	0.413	0.17	8.03	0.09

Table 4A: Comparison of WRF results with lidar measurements.

WRF & LIDAR RESULTS MACE HEAD 17H OCTOBER 2017- WIND SPEED VAD_15

MODEL	R	R	RMSE	Std Dev
WRF (25KM)	**0.97**	**0.94**	**3.13**	**0.02**
WRF (5KM)	0.96	0.92	2.07	0.02
WRF (1KM)	0.94	0.88	1.94	0.03

WRF & LIDAR RESULTS MACE HEAD 17H OCTOBER 2017- WIND SPEED VAD_75

MODEL	R	R2	RMSE	Std Dev
WRF (25KM)	0.96	0.92	3.72	0.02
WRF (5KM)	**0.96**	**0.92**	**1.98**	**0.03**
WRF (1KM)	0.93	0.87	2.16	0.03

Table 4B: Comparison of WRF results with lidar measurements.

Comparing lidar wind speed against WRF simulations on the 16 October, we can see that the agreement with wind speed VAD_15 is good (R^2 >0.59 for all WRF resolutions). The agreement with wind speed VAD_75 is poorer, (R^2 >0.41 for all WRF resolutions). The WRF 5km resolution perform' s marginally better than the 25km domain for both VAD_15 and VAD_75. This agrees with the previous in-situ 10m wind speed analysis. Comparing lidar wind speed against WRF simulations on the 17 October, we can see that the agreement with wind speed for Lidar VAD_15 & VAD_75 is excellent (R^2> 0.93) for all WRF resolutions. Again, this agrees with the in-situ 10m wind speed analysis on the 17th of October.

4.2 WRF & Lidar Wind direction vectors (30 vertical levels)

For comparison of WRF and lidar profiles of wind direction, the closest lidar altitude to the WRF levels, as well as the closest lidar time stamp to the full hour were selected. Table 4 (a & b) show comparison results for 16 & 17 October 2017 for lidar VAD_15 and VAD_75 for the u and v wind direction vectors.

WRF & LIDAR RESULTS MACE HEAD 16^{H} OCTOBER 2017- WIND DIRECTION U VECTOR VAD 15

MODEL	R	R2	RMSE	Std Dev
WRF (25KM)	0.45	0.20	11.50	0.05
WRF (5KM)	0.28	0.08	7.70	0.05
WRF (1KM)	0.50	0.25	6.50	0.05

WRF & LIDAR RESULTS MACE HEAD 16^{H} OCTOBER 2017- WIND DIRECTION V VECTOR VAD_15

MODEL	R	R2	RMSE	Std Dev
WRF (25KM)	0.61	0.37	15.70	0.04
WRF (5KM)	0.83	0.69	10.50	0.04
WRF (1KM)	0.88	0.77	8.60	0.04

WRF & LIDAR RESULTS MACE HEAD 17^{H} OCTOBER 2017- WIND DIRECTION U VECTOR VAD_15

MODEL	R	R2	RMSE	Std Dev
WRF (25KM)	0.50	0.25	4.01	0.12
WRF (5KM)	0.40	0.16	2.10	0.05
WRF (1KM)	0.50	0.25	1.90	0.04

WRF & LIDAR RESULTS MACE HEAD 17^{H} OCTOBER 2017- WIND DIRECTION V VECTOR VAD_15

MODEL	R	R2	RMSE	Std Dev
WRF (25KM)	0.95	0.90	4.30	0.02
WRF (5KM)	0.97	0.94	2.17	0.02
WRF (1KM)	0.96	0.92	2.02	0.02

Table 5: Comparison of WRF results with lidar measurements VAD_15.

Preprints (www.preprints.org) | NOT PEER-REVIEWED | Posted: 6 September 2021 doi:10.20944/preprints202109.0093.v1

WRF & LIDAR RESULTS MACE HEAD 16H OCTOBER 2017- WIND DIRECTION U VECTOR VAD 75

MODEL	R	R2	RMSE	Std Dev
WRF (25KM)	-0.42	0.18	12.7	0.04
WRF (5KM)	0.31	0.09	8.50	0.05
WRF (1KM)	0.57	0.32	6.70	0.05

WRF & LIDAR RESULTS MACE HEAD 16H OCTOBER 2017- WIND DIRECTION V VECTOR VAD_75

MODEL	R	R2	RMSE	Std Dev
WRF (25KM)	0.61	0.37	18.0	0.04
WRF (5KM)	0.82	0.67	12.3	0.03
WRF (1KM)	0.86	0.74	10.5	0.03

WRF & LIDAR RESULTS MACE HEAD 17H OCTOBER 2017- WIND DIRECTION U VECTOR VAD 75

MODEL	R	R2	RMSE	Std Dev
WRF (25KM)	0.57	0.32	4.30	0.10
WRF (5KM)	0.50	0.25	2.09	0.05
WRF (1KM)	0.60	0.36	1.88	0.05

WRF & LIDAR RESULTS MACE HEAD 17H OCTOBER 2017- WIND DIRECTION V VECTOR VAD_75

MODEL	R	R2	RMSE	Std Dev
WRF (25KM)	0.95	0.90	4.90	0.01
WRF (5KM)	0.98	0.96	2.05	0.02
WRF (1KM)	0.96	0.92	2.50	0.03

Table 6: Comparison of WRF results with lidar measurements VAD_75.

From table 5 we see that the U wind direction component agreement was poor for all days and all Lidar angles. From table 6 we see that the V wind direction component for VAD_15 and VAD_75 give similar results on both days, with good agreement on the 17th October (R^2 >0.90 for all the v vector WRF resolutions) and poorer agreement on the 16th October (R^2 >0.37 for the vector for all WRF resolutions).

We now look at the time-height plots of the relative difference in percent between WRF and lidar calculated as: *diff = 100*(X_lidar - X_wrf)/X_lidar*. We look at plots for u and v wind direction components as well as horizontal wind speed for days 16 & 17 October for Lidar angle, VAD 15.

From the Met Eireann in-situ measurements, we know that max wind speeds were detected on the 16th of October at 7:00am. On the 16th October, we can see from Figure 3, that the 5km WRF domains capture the max wind speeds seen at Mace Head at around 7:00am.

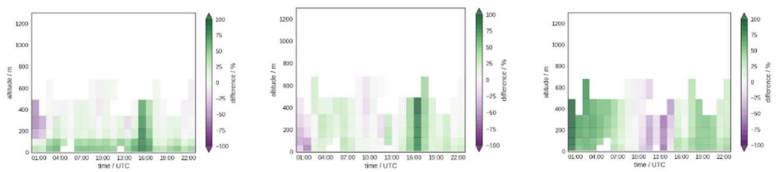

Figure 3: Wind Speed time series for % difference in Lidar and WRF 1km, 5km, 25km

In terms of wind direction on the 16th October, the u component WRF compares poorly with Lidar for all WRF resolutions, while the v component performs well in the early morning, as can be seen in Figure 4 and 5.

Preprints (www.preprints.org) | NOT PEER-REVIEWED | Posted: 6 September 2021 doi:10.20944/preprints202109.0093.v1

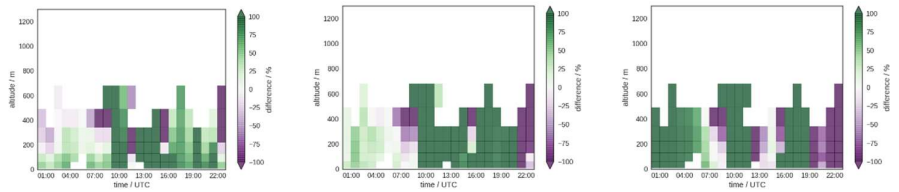

Figure 4: Time series of % difference of the u-wind component in Lidar and WRF 1km, 5km, 25km

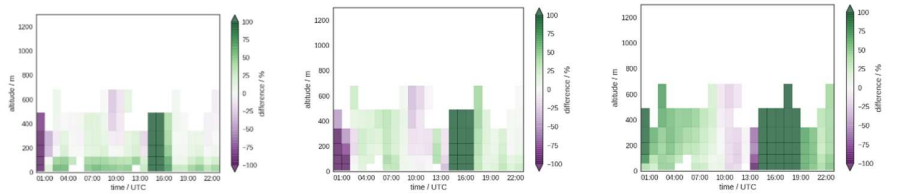

Figure 5: Time series of % difference of the v-wind component in Lidar and WRF 1km, 5km, 25km

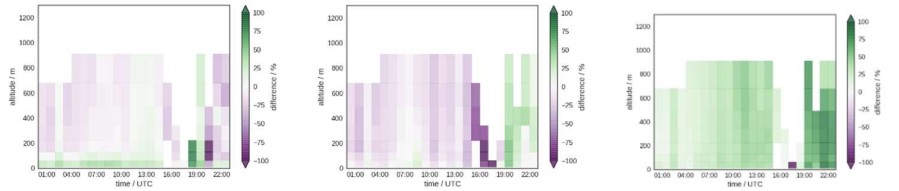

Figure 6: Wind Speed time series for % difference in Lidar and WRF 1km, 5km, 25km

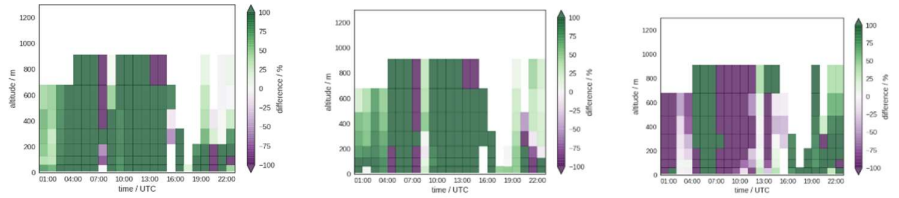

Figure 7: Time series of % difference of the u-wind component in Lidar and WRF 1km, 5km, 25km

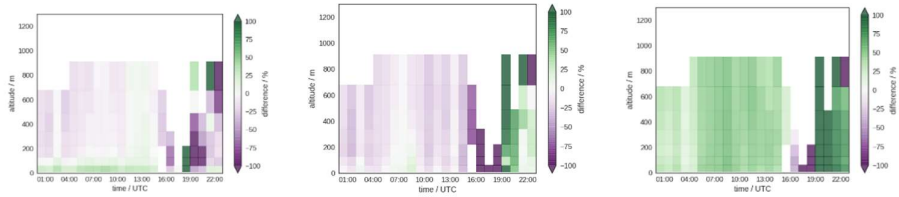

Figure 8: Time series of % difference of the v-wind component in Lidar and WRF 1km, 5km, 25km

From Figure 6, we can see that on the 17th October, the 1km WRF domain overestimates wind speed at the lower altitudes of less than 200m, while the 5km domain slightly underestimates the wind speed at less than 200m and indeed underestimates the wind speed at all altitudes in the early morning.

Here we can see that clearly the 25km domain overestimates the wind speed at all altitude, suggesting that the model performs better with a smaller domain over land, rather than a large domain which covers land and sea. The v-vector wind direction component in better agreement than the u-vector component.

Results show that as seen with the in-situ measurements, the nested 5km WRF resolution performs best for both Wind Speed and Wind Direction on the 16h & 17th October.

2 WRF Model Grid Point Analysis

The importance of selecting appropriate grid points to compare with observations is now examined in detail. The wind speed from the nearest grid point is not always the most appropriate one for this comparison, nearby ones may be more representative. To see the sensitivity of model simulation to selected grid points, we extracted the data at three grid points. One is centred at Mace Head (-9.9, 53.3), and the other two grid points are near Mace Head. One is moving towards ocean (-10.2,53.3), and the other is moving inland (-9.7,53.3).

- Mace Head centred (original)
- Mace Head, subg (inland)
- Mace Head, subo(ocean)

As Mace Head is located in the boundary of ocean and land there is a transition between two distinct surfaces which need more sub-grid points to resolve the sub-grid scale problem.

	16/10/2017			***17/10/2017***	
	Mace Head centre wind speed				
WRF resolution	R2	RMSE	MBE	R2	RMSE
25 km	0.23	3.7	-1.46	0.90	3.1
5 km	0.11	2.8	-1.45	0.93	1.6
1 km	0.17	6.1	-6.81	0.94	5.8
	Mace Head centre wind direction				
WRF resolution	R2	RMSE	MBE	R2	RMSE
25 km	0.27	35	-35	0.78	37.8
5 km	0.54	24.5	-25	0.92	11.16
1 km	0.63	14.88	-19.9	0.75	5.88

Table 7A: Comparison of WRF results with in-situ measured 10-m wind speed and direction, Mace Head centred extracted poi

	16/10/2017			***17/10/2017***	
	Mace Head subg- wind speed				
WRF resolution	R2	RMSE	MBE	R2	RMSE
25 km	0.58	3.2	-1.7	0.85	2.89
5 km	0.64	6.6	-6.4	0.63	5.38
1 km	0.78	6.2	-5.6	0.77	5.88
	Mace Head subg-wind direction				
WRF resolution	R2	RMSE	MBE	R2	RMSE
25 km	0.53	37	-40	0.75	19.57
5 km	0.68	16.33	-27	0.44	27.55
1 km	0.87	7.1	-17	0.90	23.0

Table 7B: Comparison of WRF results with in-situ measured 10-m wind speed and direction, Mace Head subg extracted point

Preprints (www.preprints.org) | NOT PEER-REVIEWED | Posted: 6 September 2021 doi:10.20944/preprints202109.0093.v1

	16/10/2017			*17/10/2017*	
	Mace Head subgo-wind speed				
WRF resolution	R2	RMSE	MBE	R2	RMSE
25 km	0.15	3.52	-0.97	0.87	3.3
5 km	0.13	9.06	-7.97	0.73	5.9
1 km	0.11	4.5	-3.07	0.77	4.6
	Mace Head subgo-wind direction				
WRF resolution	R2	RMSE	MBE	R2	RMSE
25 km	0.38	43.2	-36.0	0.88	2.8
5 km	0.7	16.5	-21.0	0.87	13.81
1 km	0.8	15.13	-16.81	0.9	19.8

Table 7C: Comparison of WRF results with in-situ measured 10-m wind speed and direction, Mace Head sub0 extracted point

From table's 7(A-C) we can see that the wind speed and direction of Mace Head Sudg performs best on the16 th October with good correlations, significantly improving (R=0.78 for WRF 1km resolution) as the grid spacing approaches 1 km. There is poor agreement for wind speed, with R^2 smaller than 0.23 for all WRF resolutions at grid point Mace Head centre and Mace Head subgo. *MBE,* however, was small. Wind direction compared better than wind speed, with R^2 larger than 0.5 for all WRF resolutions, but *RMSE* and *MBE* were large.

The comparison on the 17 th October shows excellent correlation for the Mace Head centred grid point, with wind speed correlation R^2 between 0.90 and 0.94 for all resolutions, and small *MBE* and *RMSE*. Wind direction also agreed very well, with R^2 between 0.75 and 0.92, and smaller *MBE* and *RMSE* than from the run on 16 th October.

6 WRF Model real-time Analysis & Storm tracking

In terms of local scale meteorology, we developed a unique interactive forecasting evaluation system that provides real-time, *in-situ*, observational data delivered with a range of model products to allow the viewer to discern model accuracy, and which one is performing best. Figure 9 & Figure 10 below shows the models performance during Ophelia using the real-time analysis system, three distinct models are all compared at their normal 25 km x 25 km resolution and then the nested model simulations are compared at 25 km², 5 km² and 1 km². A range of real-time meteorology data at Mace Head with a 1-minute temporal resolution is streamed and compared against the WRF model forecast.

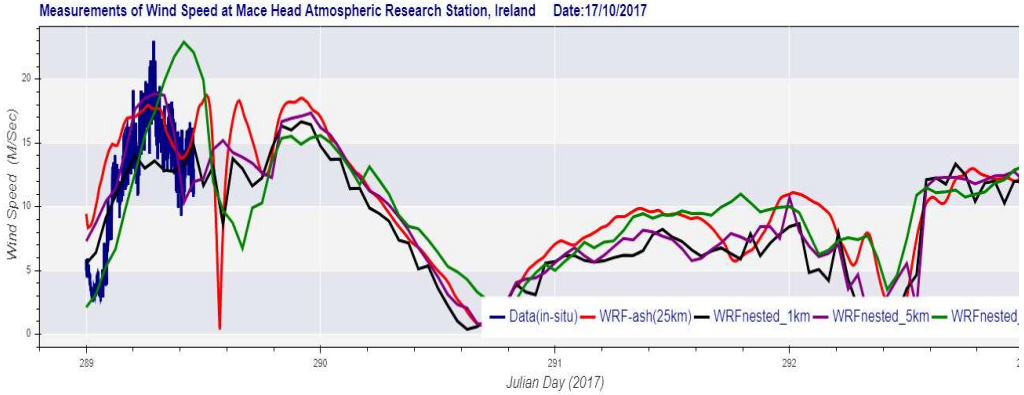

Figure 9: Real-time Analysis of WRF (25km, 5km,1km) Wind Speed during Storm Ophelia.

Preprints (www.preprints.org) | NOT PEER-REVIEWED | Posted: 6 September 2021 doi:10.20944/preprints202109.0093.v1

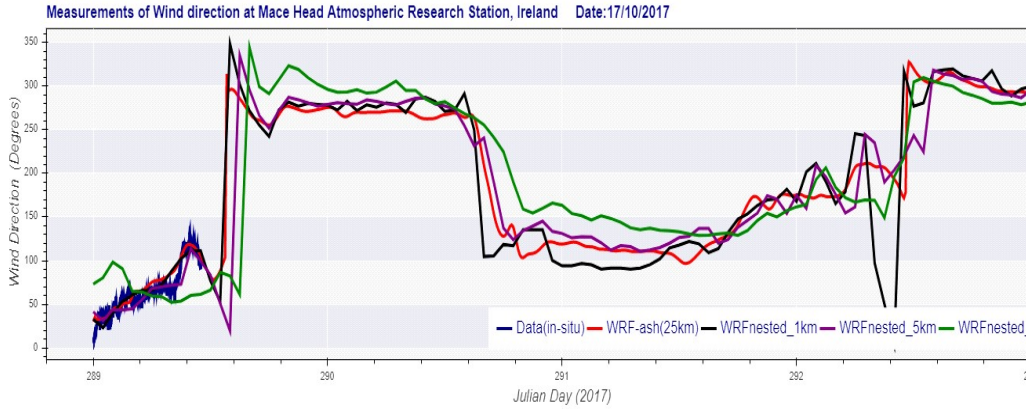

Figure 10: Real-time Analysis of WRF (25km, 5km,1km) Wind Direction during Storm Ophelia.

From Figure 9 and 10, we can see that as observed from our lidar comparison study, that the WRF 5km, appears to follow the real-time in-situ measurements at 10m best, but fails to capture the peak wind speeds. The WRF 25km showed a delay in capturing the max wind speeds and a time lag in wind direction during Storm Ophelia. While the WRF 1km, underestimates the wind speeds during Ophelia. The importance of WRF horizontal resolution is very apparent.

Finally, WRF Simulations were also evaluated in terms of their ability to track the path of Ophelia, Figure 11 show's Ophelia simulation maps from the 15th-18th October 2017. From Figure 11(A-D), you can see the track of Ophelia as it makes its way towards Ireland. The eye of the storm is clearly visible in Figure 11 (B).

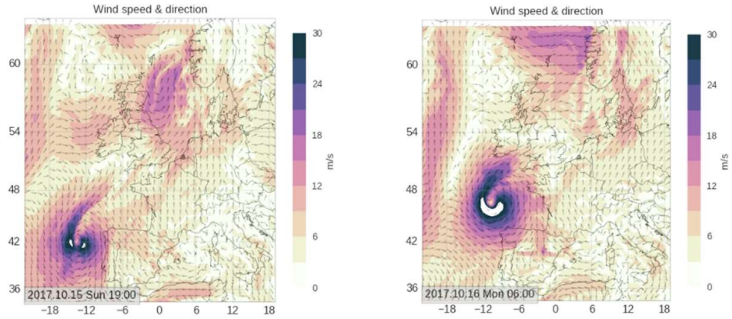

(A) Ophelia 15th October 19:00, (B) Ophelia 16th October 06:00

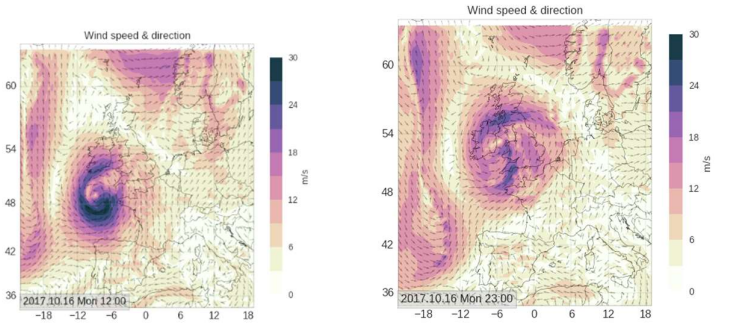

(C) Ophelia 16th October 12:00, (D) Ophelia 16th October 23:00

Figure 11(A-C): WRF Wind Speed & Direction forecast plots (A)-(F) of Storm Ophelia 15th-17th October 201

7 *Conclusions*

In this study we analysed WRF simulations during storm Ophelia, looking at key meteorological parameters, wind speed, wind direction and compared the model results against in-situ observations and remote sensing Lidar measurements at Mace Head Atmospheric research station. The model realistically simulated the magnitude and geographical distribution of the wind speed and wind direction observed during Ophelia, with good agreement with LIDAR data for both wind speed and direction on the 16th October and excellent agreement with wind speed and direction on the 17th October (R^2>0.9 for the WRF 25km domain and the 5km domain). The model simulation showed to have generally small biases in the simulated wind speed and wind direction during this case study.

The importance of selecting representative grid points for evaluating the model performance has also been shown to be of relevance at Mace Head. As Mace Head is located in the boundary of ocean and land there is a transition between two distinct surfaces which need more sub-grid points to resolve the sub-grid scale problem. We can see from our study that moving the grid inland (Mace Head Sudg) increases the performance of the model during Ophelia (16 th October) with good correlations (R^2 >0.58) for wind speed, with good correlations (R^2=0.78 for WRF 1km resolution) as the grid spacing approaches 1 km. Wind direction also correlated well, with R^2 >0.53 for all WRF resolutions, with excellent correlation (R^2 =0.87) as the resolution increases to 1km.

From this study, the correct choice of model resolution becomes apparent, we can see that the WRF 25km has a delay in capturing the max wind speeds and a time lag in wind direction. Results show that as seen with the in-situ measurements, the nested 5km WRF resolution performs best for both Wind Speed and Wind Direction on the 16h & 17th October, the model's capability to forecast extreme weather events such as Storm Ophelia is of upmost importance and now with a changing climate, it becomes more important to improve and enhance model forecasting capability.

Acknowledgments

This work was funded by Science Foundation Ireland for MaREI, the SFI Research Centre for Energy, Climate and Marine, and the Irish Centre for High-End Computing (ICHEC). The Doppler wind LIDARs are property of Irish Aviation Authority.

References

1. IPCC, 2021: Climate Change 2021: The Physical Science Basis. Contribution of Working Group I to the Sixth Assessment Report of the Intergovernmental Panel on Climate Change [Masson-Delmotte, V., P. Zhai, A. Pirani, S. L. Connors, C. Péan, S. Berger, N. Caud, Y. Chen, L. Goldfarb, M. I. Gomis, M. Huang, K. Leitzell, E. Lonnoy, J. B. R. Matthews, T. K. Maycock, T. Waterfield, O. Yelekçi, R. Yu and B. Zhou (eds.)]. Cambridge University Press. In Press.
2. Otto, F.E.L., Philip, S., Kew, S. *et al.* Attributing high-impact extreme events across timescales—a case study of four different types of events. *Climatic Change* **149,** 399–412 (2018).
3. Yamada, Y., K. Oouchi, M. Satoh, H. Tomita, and W. Yanase (2010), Projection of changes in trop-ical cyclone activity and cloud height due to greenhouse warming: Global cloud- system- resolving approach, Geophys. Res. Lett., 37,L07709, doi:10.1029/ 2010GL042518.
4. U.S. CLIVAR Hurricane Workshop report, Rep. 2013-5, 18 pp., U.S. CLIVAR Proj. Off., Washington, D. C
5. Knutson, T. R., J. J. Sirutis, G. A. Vecchi, S. Garner, M. Zhao, H.-S. Kim, M. Bender, R. E. Tuleya, I. M. Held, and G. Villarini (2013), Dynamical down-scaling projections of twenty- fi rst- century Atlantic hurricane activity: CMIP3 and CMIP5 model-based scenarios, J. Clim., 26, 6591–6617, doi:10.1175/ jcli-d-12-00539.1.
6. Frank WM, George SY. The interannual variability of tropical cyclones. Mon. Wea. Rev. 2007;135:3587–3598.
7. Raju, P.V.S., Potty, J. & Mohanty, U.C. Meteorol Atmos Phys (2011) 113: 125. https://doi.org/10.1007/s00703-011-0151-y

8. Li, X., and Z. Pu, 2008: Sensitivity of numerical simulation of early rapid intensification of Hurricane Emily (2005) to cloud microphysical and planetary boundary layer parameterizations. Mon. Wea. Rev., 136, 4819–4838
9. Borge, R., V. Alexandrov, J. J. del Vas, J. Lumbreras, and E. Rodriguez, 2008: A comprehensive sensitivity analysis of the WRF model for air quality applications over the Iberian Peninsula. Atmos. Environ., 42, 8560–8574.
10. Skamarock, W.C.; Klemp, J.B.; Dudhia, J.; Gill, D.O.; Barker, D.M.; Duda, M.G.; Huang, X.-Y.; Wang, W.; Powers, J.G. A Description of the Advanced Research WRF Version 3; NCAR Technical Note: NCAR/TN-4751+STR; National Center for Atmospheric Research: Boulder, CO, USA, 2008.
11. Dodla VB, Desamsetti S, Yerramilli A. A comparison of HWRF, ARW and NMM models in Hurricane Katrina (2005) simulation. Int J Environ Res Public Health. 2011;8(6):2447–2469. doi:10.3390/ijerph8062447
12. Jiménez, P.A. and J. Dudhia, 2012: Improving the Representation of Resolved and Unresolved Topographic Effects on Surface Wind in the WRF Model. J. Appl. Meteor. Climatol., 51, 300–316, https://doi.org/10.1175/JAMC-D-11-084.1
13. Davis C, Wang W, Chen SS, et al. Prediction of Landfalling Hurricanes with the Advanced Hurricane WRF Model. Monthly Weather Review. 2008;136(6):1990-2005. doi:10.1175/2007MWR2085.1.
14. Jiménez, P.A. and J. Dudhia, 2012: Improving the Representation of Resolved and Unresolved Topographic Effects on Surface Wind in the WRF Model. J. Appl. Meteor. Climatol., 51, 300–316, https://doi.org/10.1175/JAMC-D-11-084.1
15. Done, J.M., Holland, G.J., Bruyère, C.L. et al. Climatic Change (2015) 129: 381. https://doi.org/10.1007/s10584-013-0954-6
16. Dodla VB, Desamsetti S, Yerramilli A. A comparison of HWRF, ARW and NMM models in Hurricane Katrina (2005) simulation. Int J Environ Res Public Health. 2011;8(6):2447–2469. doi:10.3390/ijerph8062447
17. Das, Ananda & Rao, Y. & Tallapragada, Vijay & Zhang, Zhan & Bhowmik, S. & Sharma, Arun. (2015). Evaluation of the Hurricane Weather Research and Forecasting (HWRF) model for tropical cyclone forecasts over the North Indian Ocean (NIO). Natural Hazards. 75. 10.1007/s11069-014-1362-6.
18. Floors, R., Batchvarova, E., Gryning, S-E., Hahmann, A. N., Pena Diaz, A., & Mikkelsen, T. (2011). Atmospheric boundary layer wind profile at a flat coastal site – wind speed lidar measurements and mesoscale modeling results. Advances in Science and Research, 6, 155-159. https://doi.org/10.5194/asr-6-155-2011
19. O'Connor, T.C. and Sharkey, W.P.F. (1960)- Ionization equilibrium in maritime air, Proc. Roy. Ir. Acad., 61, p.15-27.
20. Heard, D. E.et al, The North Atlantic Marine Boundary Layer Experiment (NAMBLEX). Overview of the campaign held at Mace Head, Ireland, in summer 2002, Atmos. Chem. Phys., 6, 2241-2272, 2006.
21. Mlawer, E. J., S. J. Taubman, P. D. Brown, M. J. Iacono, and S. A. Clough (1997),586 Radiative transfer for inhomogeneous atmospheres: RRTM, a validated correlatedk587 model for the longwave, Journal of Geophysical Research, 102, 16,663–16,682, doi:588 10.1029/97JD00237
22. Berrisford, P., D. P. Dee, P. Poli, R. Brugge, M. Fielding, M. Fuentes, P. W. Kallberg,517 S. Kobayashi, S. Uppala, and A. Simmons (2011), The ERA-Interim archive Version 2.0,518 ECMWF ERA Report Series No.1 Version 2.0
23. Lin, Y.-L., R. D. Rarley, and O. H. D. (1983), Bulk parameterization of the snow field579 in a cloud model, Journal of Applied Meteorology, 22, 1065–1092, doi:10.1175/1520-580 0450(1983)022¡1065:BPOTSF¿2.0.CO;2
24. Arakawa, A., and V. R. Lamb (1977), Computational design of the basic dynamical pro-502 cesses of the UCLA general circulation model, Methods in Computational Physics:503 Advances in Research and Applications, 17, 173–265, doi:10.1016/B978-0-12-460817-504 7.50009-4
25. Hong, S., Y. Noh, and J. Dudhia (2006), A new vertical diffusion package with an ex-552 plicit treatment of entrainment processes, Monthly Weather Review, 134, 2318–2341,553 doi:10.1175/MWR3199.1
26. Davis, C., Wang, W., Chen, S. S., Chen, Y., Corbosiero, K., DeMaria, M., ... Xiao, Q. (2008). Prediction of landfalling hurricanes with the advanced hurricane WRF model. *Monthly Weather Review*, *136*(6), 1990-2005.
27. Davis, C.; Wang, W.; Chen, S.S.; Chen, Y.; Corbosiero, K.; DeMaria, M.; Dudhia, J.; Holland, G.; Klemp, J.; Michalakes, J.; et al. Prediction of landfalling hurricanes with the advanced hurricane WRF Model. Mon. Weather Rev. 2008, 136, 1990–2005.
28. Bao JW, Michelson SA, Persson POG, Djalalova IV, Wilczak JM., Observed and WRF-simulated low-level winds in a high-ozone episode during the Central California Ozone Study. J. Appl. Meteor. Climatol. 47: 2372–2394, 2008.
29. Hu X.-M., J. W. Nielsen-Gammon, and F. Zhang, "Evaluation of three planetary boundary layer schemes in the WRF model," Journal of Applied Meteorology and Climatology, vol. 49, no. 9, pp.1831–1844,2010.
30. Nunalee CG and Basu S, Mesoscale modelling of coastal low-level jets: implications for offshore wind resource estimation. Wind Energy 17:1199–1216, 2014.
31. Skamarock WC, Klemp JB, Dudhia J, Gill DO, Barker DM, Duda MG, Huang XY, Wang W, Powers JG. A description of the advanced research WRF version 3. Technical Report NCAR/TN-457+STR, National Center for Atmospheric Research, 2008.
32. Storm B, Dudhia J, Basu S, Swift A, Giammanco I., Evaluation of the Weather Research and Forecasting model on forecasting low-level jets: Implication for wind energy. Wind Energy 12: 81–90, 2009.
33. Browning, K. A., and R. Wexler (1968), The Determination of Kinematic Properties of a Wind Field Using Doppler Radar, Journal of Applied Meteorology, 7, 105–113, doi: 10.1175/1520-0450(1968)007¡0105:TDOKPO¿2.0.CO;2.
34. Murphy, A. H., 1991: Probabilities, odds, and forecasts of rare events. Wea. Forecasting, 6, 302–307, https://doi.org/10.1175/1520-0434(1991)006,0302:POAFOR.2.0.CO;2.